SlyD accelerates *trans*-to-*cis* prolyl isomerization in a mechano-signaling protein under load

Abhigyan Sengupta[1, ‡], Lorenz E. Rognoni[1, ‡], Ulrich Merkel[1], Gabriel Žoldák[2] and Matthias Rief[1,*]

KEYWORDS

Single-molecule force spectroscopy (SMFS), Optical tweezers, Peptidyl-prolyl isomerase, SlyD, Filamin, *trans-cis* isomerization, constant velocity pulls, constant distance, jump experiment

ABSTRACT

Prolyl isomerization is recognized as one of the key regulatory mechanisms, which plays crucial role in cell signaling [1], ion channel gating [2], phage virus infection [3] and molecular timing[4]. This kind of isomerization is usually slow, but can be accelerated by peptidyl-prolyl isomerases (PPIase). Using single molecule force spectroscopy, we have shown that cytoskeletal mechano-sensing protein filamin domain 20 (FlnA20) contains highly conservative proline residue, P2225, which is in the native state of FlnA20 interconverts between *cis-trans* isomers. In this paper we asked, whether the native-state isomerization of the filamin protein under force can be catalyzed by PPIases. As a model enzyme, the highly active bacterial PPIase SlyD(1-165) was used, which is from FK506-binding protein (FKBP) class of PPIases. To explore the catalysis and binding of the enzyme to FlnA20, we have used several experimental protocols, e.g., constant velocity,

constant distance, and jump experiments. Our results show that in the presence of super-stoichiometric SlyD concentration, the *trans*-to-*cis* isomerization rate is more than 25-fold accelerated compared to the non-enzymatic reaction. A concentration-dependent depletion of the *trans*-isomer lifetime was observed. Additionally, we observed that SlyD binds to the *cis*-isomer of the native state of FlnA20, while stabilizing the FlnA20-SlyD complex by ~2 k_BT. This is the first single-molecule observation of catalysis of the *cis*/*trans* isomerization process by a PPIase in a mechano-protein.

INTRODUCTION

Protein folding is a complex search process on a high-dimensional energy surface.[5] Even though protein folding can, in some cases, occur spontaneously, nature has developed machinery of helper proteins supporting this folding process.[6] Recently, it has been observed that *cis-trans* isomerization of a particular amino acid, proline, in a native protein can significantly impact its structure and function.[7] Such an intra-protein conformational change resulted from peptidyl-prolyl *cis-trans* isomerization is gaining significant attention as a new regulatory mechanism.[7]

A few but intriguing examples of prolyl *cis-trans* isomerization regulated processes are cell signaling [1], ion channel gating [2], phage virus infection [3], and molecular timing [4]. The *cis* and *trans* isomers of free proline in solution are almost isoenergetic, which allows proline to exist in either of the isomeric forms with equal probability. It's reported that X-Pro (X being any amino acid but proline) in small peptides and unfolded protein equally or nearly equally populates both of the isoenergic *cis* and *trans* isomers, with a marginally higher weightage to the *trans* isomer, due to a small difference of Gibbs free energy (<8 kJ/mol) between the two states. [8] This non-

preferential selection of proline isomers in solution is invalidated when proline resides inside protein pockets. Proline residue in native proteins can exist exclusively, either *cis* or *trans* isomer, due to favorable neighboring group interactions between surrounding amino acids and X-Pro. [9] Although most of the native proteins consist of *trans* proline, a number of examples with *cis* proline isomer [10] and a few native proteins containing both *cis* and *trans* proline isomers are also known [11]. The biologically active structure of the native protein is sensitive to the involved proline isomer and, in most cases, tries to fold in a correct fashion by passing through a rate-limiting peptidyl-prolyl *cis-trans* isomerization step. Due to a high activation energy barrier (~60-80 kJ/mol)[10d] in native proteins, peptidyl-prolyl *cis-trans* isomerization happens slowly at equilibrium. To control and regulate such a slow process, a specific class of enzymes exists called peptidyl-prolyl isomerase (PPIase). Quantitative information on individual enzymatic steps is scarce about the peptidyl-prolyl *cis-trans* isomerization activity and its impact on different protein folding pathways. In one such study, Žoldák *et al.* reported an FKBP enzyme that catalyzes conformational folding of ribonuclease T1 protein, using stopped-flow kinetic measurement. They observed ~10^4 times accelerated prolyl *cis-trans* isomerization rate in the presence of the enzyme SlyD. [12]

In the current study, we investigated the thermodynamic and kinetic influences of a bacterial peptidyl-prolyl isomerase, SlyD, on the proline (P2225) in an isolated human FilaminA domain 20 (FlnA20) as a substrate. Several studies have also shown Filamin as a mechano-signaling hub in the cytoskeleton, which participates in the interaction to transmembrane receptors like integrin or the von Willebrand receptor glycoprotein Ib (GPIb).[13] Particularly, Filamin is chosen as the model substrate in the current study because Filamin A domain 20 (FlnA20) contains a native *cis* proline residue close to the protein surface in front of the last B-strand (Figure 1a).

This *cis* proline is strictly conserved in all naturally occurring filamin Ig-like domains.[14] Using single-molecule force spectroscopic techniques, our group showed that this particular proline (P2225) in Filamin-A20 exhibits a native state peptidyl-prolyl isomerization, with some prolonged isomeric lifetimes (typically in minutes).[14] It is intuitive to choose such a protein to explore the influence of PPIs, as it already has well-characterized thermodynamic and kinetic properties. Single-molecule force spectroscopy with optical tweezer provides the opportunity to study the proline *cis-trans* isomerization under the influence of a peptidyl-prolyl isomerase (PPIase), which is for the first time reported here on a single molecule level. From our experiments, we find a significant acceleration of the *trans* to *cis* isomerization and a concentration dependent binding interaction by the bacterial PPI, SlyD. We have also observed an increased stability of ~2 k_BT of the native state of FlnA20, which originates from the binding process of the protein presumably due to chaperone activity of the enzyme.

MATERIALS AND METHODS

1. Optical Trap Setup

A custom-built optical tweezers setup is used for the single-molecule force measurements. A detailed description of the setup is already given in our previous publications.[13c, 14] In short, the trap has a dual-beam design with one AOD-steerable beam and a back focal plane detection. Trapped beads were calibrated with the technique reported by Toli´c-Nørrelykke *et al.* [15] The trap stiffness was determined with an error of approximately 10%, and force sensitivity varied between different experiments from 0.25-0.3 pN/nm. All data acquisition was done at a sampling rate of 100 kHz and averaged to 20 kHz before storage. For data analysis, the difference of both bead signals was calculated after the experiment in order to increase the signal-to-noise ratio.[16] The

signals were corrected for both crosstalk due to depolarization and proximity of the trapping beams. For computational reasons, long passive-mode collections of equilibrium time traces with slow kinetics (e.g. the un-catalysed *cis-trans* isomerization) were analysed after resampling to 5 kHz.

2. The Dumbbell Assay

The dual-beam design of the optical tweezers setup was used in a dumbbell geometry for force applications, as shown in Figure 1a. Special molecular constructs are designed by tethering the protein termini to a 544 base pair long double-stranded DNA oligonucleotides through a strain-promoted azide-alkyne (copper free) Click Chemistry (SPAAC). The ends of the DNA were functionalized with biotin and digoxigenin, respectively, which are used in attachment to 1μm diameter silica beads, together resulting in a dumbbell shape to the stretched bead-DNA-protein-DNA-bead construct. [17] The DNA molecules as handles separate the investigated protein from the bead surface and the trapping lasers. This geometry helps in reducing the heating of the protein and prevents undesired surface reactions as well as photochemical damages. Furthermore, all protein constructs are inserted between two ubiquitin domains with terminal cysteine using molecular cloning techniques and expressed in *E-coli*. The ubiquitins serve as spacer molecules during construct production to prevent direct reaction of the terminal cysteine later used for DNA-handle coupling. Because ubiquitin domains are mechanically much more stable than the target protein, they do not unfold at our exerted force range and, thus, do not interfere during the single-molecule mechanical measurements. [14]

For a successful construct formation, one protein needs to bind two 544 bp long double-stranded DNA handle molecules. Because attachment of the second DNA molecule was drastically

hindered by the electrostatic repulsion of the already bound DNA, we only used short single-stranded DNA oligonucleotides. The terminal cysteine of the protein construct was activated by dithiodipyridine and mixed with tris (2-carboxyethyl) phosphine-activated 3′ thiol groups of 34-bp ssDNA oligos. Double-stranded DNA molecules were produced by Polymerase Chain Reaction (PCR) on a lambda phage template. The sense primers were triply functionalized with biotin or digoxigenin, while the antisense primers contained an abasic site that caused the polymerase to fall off and left a single-stranded overhang. Finally, this overhang was hybridized to the protein-coupled DNA oligos, which resulted in the complete DNA-protein-DNA construct. The choice of the bead size was a trade-off between good experimental handling, high visibility in the bright field of the setup, and good trapping behaviour as well as low hydrodynamic drag. As bead material, we prefer silica over polystyrene because of the distinct advantage of reduced sample heating[18] and lower damage to the sample due to the creation of free oxygen radicals[19]. This resulted in choosing silica beads with a diameter of 1 μm.

3. Bacterial SlyD

In this study, SlyD, a member of the FKBP family, was used as a model PPIase. The two-domain protein SlyD of *Escherichia coli* functions as a molecular chaperone, a prolyl *cis* - *trans* isomerase, and a nickel-binding protein.[20] Figure S1 shows a solution structure (PDBid: 2K8I) of SlyD with the chaperone domain (60 residues) being coloured in blue and the FKBP-like isomerase domain (90-residues) being coloured in red. [21] In human FKPP12 β-strands 2 and 3 are connected by a loop, which is called the flap. Hence, in SlyD, the inserted chaperone domain is also known as the insert-in-flap (IF) domain. The FKBP domain of SlyD is a structural homolog of human FKBP12. In addition to the well-structured two domains, wild type SlyD from *Escherichia coli* also has a

C-terminal disordered 40 residues long histidine-rich tail that can bind up to 7 nickel ions.[22] In the presence of metal ions, this tail interferes with the isomerase activity of SlyD and can reduce the in vitro solubility. For the current work, only the well-studied [23] shortened version SlyD was used, which lacks the disordered tail (**Figure S1**).

4. Measurement Protocols

In the current experiments, mainly three types of experimental protocols are used: (a) constant velocity, (b) constant distance (also mentioned as equilibrium measurement), and (c) jump experiments.

(a) Constant velocity experiments

Constant-velocity experiments are useful for quickly assessing the general force scales for folding and unfolding. In a typical constant velocity experiment, as shown in Figure 1a, the mobile trap moves back and forth from the fixed trap with a constant velocity ranging from typically 10 to 500 nm/s. The force generated along the pulling direction stretches the DNA and destabilizes the protein until one domain unfolds, which causes a length increase of the stretched construct and a decrease of the applied force due to bead relaxation in the trapping potentials (Figure 1b). From the length increase, the number of amino acids involved in the unfolding transition can be obtained with high precision. Usually, the trap centers are approached again, and, depending on the studied protein, a refolding against force can be observed. This stretch-and-relax cycle (Figure 1b) is then repeated many times. The unfolding forces are distributed depending on the unfolding rate constant and the position of the transition state. This information can be obtained by analysing the pulling

speed dependence of the peak of these unfolding force distributions. Various models have been suggested to extract energy landscape information from these data. [24]

During constant-velocity experiments, force vs. extension curves were recorded, as shown in Figure 1b. The curve shape can be reproduced with a model describing the elasticity of a DNA-protein chain. For the low force regime, where the protein is still folded and all tethered ligands bound, we model the DNA handle elasticity with an extensible worm-like chain model (eWLC).[17a] In this model, the force is given by;

$$F_{eWLC}^{dDNA} = \frac{k_B T}{\rho_{DNA}} \left(\frac{1}{4\left(1-\frac{d_{DNA}}{L_{DNA}}+\frac{F}{K}\right)^2} - \frac{1}{4} + \frac{d_{DNA}}{L_{DNA}} - \frac{F}{K} \right) \quad (1)$$

with persistence length ρ_{DNA}, contour length L_{DNA}, elastic modulus K and extension d_{DNA}. The fit yielded persistence lengths of approximately 20 nm, contour lengths of approximately 360 nm, and elastic moduli of approximately 600 pN. The force-induced unfolding of the protein adds a flexible polypeptide chain to the compliance of the DNA-protein construct. We account for this by applying the eWLC describing the DNA with the previously determined parameters in series to a worm-like chain model (WLC) [25] for the unfolded protein;

$$F_{WLC}^{d_{prot}} = \frac{k_B T}{\rho_{prot}} \left(\frac{1}{4\left(1-\frac{d_{prot}}{L_{prot}}\right)^2} - \frac{1}{4} + \frac{d_{prot}}{L_{prot}} \right) \quad (2)$$

with persistence length ρ_{prot} set to 0.7 nm, contour length L_{prot} and extension d_{prot}.

(b) Constant distance experiments (equilibrium measurements)

In these experiments, the two trap centers are held at a constant separation, thus applying a quasi-constant force bias to the dumbbell. Due to the length change caused by unfolding or folding of the investigated protein and the coupled bead relaxation in the non-linear trap potentials, this force bias will be higher for the folded than for the unfolded protein. A theoretically more direct approach is a constant force experiment, where a feedback loop maintains a constant force over time. Because of the response time of this active force stabilization (>1 ms), the force cannot be held constant during the ~ms timescale occurring in folding/unfolding transitions. Hence, in optical tweezers experiments, it is more advantageous to use the constant distance approach over a force clamp approach.

For the constant distance mode used in this study (Figure 1c, Figure 2), both beads were positioned in the linear regime of the trapping potential. This gives the best force and time resolution due to a higher effective trap stiffness compared to the passive force clamp mode. In Figure 1c, a time trace of a typical passive-mode experiment at a biasing force ~4.9 pN is shown in the presence and absence of SlyD. The extracted population probabilities and dwell time distributions of the levels are used to calculate equilibrium free energies and force-dependent microscopic kinetic rate constants. Hidden Markov models and pair-correlation analysis[26] were used for quantitative analysis. To extract kinetic and equilibrium parameters approaching zero force, all elastic contributions from the trap spring constants, as well as the DNA and protein spacers, have to be considered.

(c) Jump experiments

In many cases, the folding and unfolding rates were too slow to gather significant statistics in the experimental time range. A jump protocol was used to speed up the kinetics in these cases, in that the protein is cycled between two force biases.[27] At higher forces, the protein unfolding accelerated while lower forces promote the folding, which is shown in Figure 3. In contrast to the equilibrium approach, now, only one folding direction was observed per jump level (unfolding for a high force bias and folding for a low biasing force). The other direction was drastically slowed down and, therefore became unmeasurable. From the folded dwell times at the high force bias, the unfolding rates are determined by fitting a single exponential to the accumulated dwell times histogram. At the same time, the unfolded dwell times at low biasing force give the folding rate in the same way. The protein folding process can be described as a diffusion process in a potential. [28] In the over-damped case, the fate of the transition is independent of what happened before, resulting in a memoryless process known as a Markov process. Therefore, the jump dwells can also be shorter than a typical dwell time. In the case of the high force bias, the folded dwell times were summed up until the first unfolding takes place and vice versa for the lower force bias.

For FlnA20 we used the following jump experiment protocol, as shown in Figure 3, panel1. Starting with the protein in the native F(*cis*) state, the trap separation is increased within 10 μs (black "I" in Figure 3) and a force bias between 15 and 25 pN is applied to the folded domain. As a result, the F(*cis*) goes to a U(*cis*/*trans*) state, where the assignment of the unfolded state to a *cis*/*trans* is not possible, when the protein does not undergo transitions between unfolded-*cis* and unfolded-*trans* states. After a fixed period of time, the protein is relaxed (black "II" in Figure 3, panel1) to a low force around 4 pN, where the isomerization state can now be detected. Depending

on whether the proline switched to the *trans* isoform, the protein can show two distinct behaviours; (i) a series of unfolding and folding events within the *trans* state (highlighted by the magenta box), (ii) a single step folding corresponding to the *cis* state (after the magenta box). In case (i) when the *cis*-*trans* isomerization takes place, the protein will rapidly fluctuate between the unfolded and folded states (F/U(*trans*)) and the measured folding and unfolding dwell times are used to determine the *trans* unfolding and folding rates. After a while the fluctuation stops because the prolyl bond switches back to the *cis* state, which "locks" the protein in folded *cis* configuration as mentioned in option (ii). To "unlock" the protein from folded-*cis* configuration, the force-bias is again increased (black "III" in Figure 3a) leading to the unfolding of the protein. These steps from I-III are repeated multiple times to generate the cumulative distributions of the dwell times and hence the corresponding rate constants. More details of the jump assay analysis techniques are mentioned elsewhere. [14]

RESULTS

(A) Single-molecule Proline switching without isomerase

The force-dependent proline isomerization kinetics in the absence of isomerase has been studied [14] in detail before, and here we briefly summarize those results to compare them later to the isomerase-dependent kinetics. To study the force-dependent folding-unfolding dynamics of Filamin A domain 20 (FlnA20) in the absence of the isomerase SlyD, we used a construct, where only domain FlnA20 is sandwiched between two ubiquitin molecules (Figure 1A) and attached to the double-stranded DNA handles (See method section). Then the DNA-FlnA20-DNA construct was attached to the beads using specific non-covalent interactions, leading to the dumbbell configuration used in our optical tweezers experiment (Figure1a). The ubiquitins at either side of

the Filamin-A20 (FlnA20) work as a spacer domain, which doesn't unfold at the forces used in our assay.[17c]

To explore the unfolding and folding behaviour of the FlnA20, we first utilized the constant velocity cycles (see method section), where one trap is kept fixed and the other trap moves back and forth, with constant speed (500 nm/s and 100 nm/s) (Figure 1b) resulting in folding and unfolding of the target protein FlnA20. A series of subsequent stretch (deep brown) and relax (light brown) cycles are collected from a single FlnA20 domain. Some of the representative time traces are shown in Figure 1b. The switching between the folded and the unfolded state is reversible with the molecule refolding in every relax cycle. In each stretch cycle, an unfolding event can be observed; however, the forces either scatter around a low value near 5 pN or around a higher value near 15 pN. Refolding events occur at forces around 3 pN in all the relaxation cycles (Figure 1b, light brown). The distributions of the unfolding forces are given in the left hand histogram in figure 1b, which shows that the observed unfolding events clearly fall into two distinct classes, one at 5 pN and another at 15 pN. Every unfolding event at higher or lower forces exhibits the same contour length increase, which is around 23 nm for FlnA20. This bimodal force distribution of FlnA20 unfolding can be linked to a *cis-trans* isomerization of P2225 (Figure 1a), with the *trans* isoform leading to low unfolding forces and the *cis*-isoform high unfolding forces. [14]

The change in stability of the folded protein is linked to the isomerization state of P2225 and can now be used as a readout to observe the kinetics of the *cis-trans* isomerization in real-time. Single-molecule experiments performed in equilibrium mode (Figure 1c) were performed holding both traps at a constant distance (see method section). During this measurement, a single FlnA20 molecule undergoes many transitions between the folded (purple) and the unfolded (red) state. Two alternating regimes can be observed (see grey shaded bar above Figure 1c); (i) an

unstable regime, where the unfolded state dominates with only a few short-lived refolding events (short spikes). This regime reflects the *trans* state of P2225[14] (marked in dark grey above the trace). (ii) A stable regime, where the molecule is predominantly folded (purple state) with only a few excursions to the unfolded state. This regime reflects the *cis* state of P2225 [14] (marked in light grey above the trace). Note that both the folded and the unfolded states are populated in both the *cis* and *trans* isoforms, however, with a drastically different population probability reflecting the different stabilities of the folded state. Hence four different interconnected states; two native states (*trans* (N_{trans}) and *cis* (N_{cis})) and two unfolded state (*trans* (U_{trans}) and *cis* (U_{cis})) can be discerned, which are also depicted together in the four state kinetic model in Figure 1d. A detailed thermodynamic and kinetic description of these states has been performed and reported by us previously.[14] In the following, we will use the kinetic information of the four-state model (Figure 1d) from that study.[14]

(B) Single-Molecule observation of isomerase catalysed *cis*/*trans* kinetics

The results of single-molecule equilibrium experiments with increasing concentrations of SlyD is shown in Figure 2. To omit force-induced effects on the folding-unfolding dynamics, the force bias (mentioned at the top right corner of each of the time traces) is kept similar for different concentrations of SlyD (mentioned at the top left corner of each of the time traces). The respective force and time scaling are marked at the bottom left side of each panel. The top panel represents the no-SlyD condition, where the *cis* and *trans* states' duration are marked at the top of the panel by light and dark grey, respectively. As described above, we can observe transitions between 2 regimes: the *cis*-isomer with predominantly folded (purple) states interspersed by only a few short-lived unfolded states (red) and the *trans* isomer regime, with mostly unfolded protein and only a

few short-lived refolding events. The second panel shows an equilibrium trace in the presence of 0.0145 μM SlyD, which approximately has two times higher number of transitions between the *cis* (light grey) and *trans* (dark grey) regimes, compared to the no SlyD condition. Increasing the concentration of SlyD by 50 times (0.725μM, panel 3) compared to the previous 0.0145 μM of SlyD shows, at first sight, a surprising result is observed; the number of transitions seems significantly less compared to the 0.0145 μM SlyD. Moreover, the *cis* states seem to be significantly more populated than the *trans* states. Apparently a clear separation between *cis* and *trans* isomeric states cannot be performed anymore because lifetimes of the unfolded state of the protein become similar to the *cis*-*trans* isomerization kinetics. Therefore, we cannot assign the *cis* and *trans* regimes anymore. This observation becomes even more drastic in the presence of 7.25 μM SlyD. At this high concentration, it appears as if the enzyme is not just acting as an enzyme but also pushes the equilibrium towards the *cis* folded state, possibly by direct interaction with the folded protein. Apparently, the constant force assay does not provide a good enough time resolution to follow the switching kinetics at higher SlyD concentrations.

To better understand the effect of SlyD on FlnA20, and to extract the kinetic information in the presence of SlyD, we next performed jump experiments (Figure 3), where the assay is an analogy to double-jump bulk experiments. [29] A detailed description of these experiments is given in the method section. In brief, in a jump experiment starting out in the folded *cis* state, the trap separation is increased rapidly (less than 10 μs) applying a force between 15 and 25 pN to the *cis*-folded domain (Figure 3a, marked as F(*cis*)) until unfolding happens (Figure 3a, marked as U(*cis*/*trans*)). After the protein unfolds, it will eventually transition to the *trans*-unfolded state. After a rapid quench to a low force ~5 pN, the *trans* state manifested itself in a rapid

folding/unfolding equilibrium (see magenta-coloured box in Figure 3a upper panel, as well as in the zoomed section below). The rapid folding/unfolding equilibrium lasted until an isomerization event drives the protein into its much more stable *cis* state, which readily locked into the folded state, where it remained for the rest of the low force quench time. The data in Figure 3a shows a jump experiment for the no SlyD condition. These results in the absence of SlyD are consistent with our previous work[14] showing effective *trans*-to-*cis* isomerization rates in the range 0.05/s. With increasing concentration of SlyD those isomerization rates increase drastically, and the *trans* state switches to the *cis* state already within seconds at the highest SlyD concentrations (see Figure 3b and 3c). Apparently, our jump assay has increased the time resolution in the desired way and shows a clear catalytic effect of SlyD across all concentrations used.

Plotting the observed *trans-cis* isomerization rates yield isomerization rate as a function of enzyme concentration (Figure 3d). It is important to note that well-known Michaelis-Menten kinetics observed in bulk experiments are not valid in this single-molecule experiment because we do not vary substrate concentration but instead use a single substrate molecule and vary the enzyme concentration; hence the situation can be approximated by the reverse quasi-steady-state assumption. [30]

Therefore, our results can be modelled by a binding model, which utilizes binding probabilities for the enzyme to its substrate;

$$k_{tc}^{eff}[SlyD] = k_{tc}^{app}.(1 - P_{bound})[SlyD] + k_{tc}^{app,SlyD}.P_{bound}[SlyD] \quad (3)$$

Here k_{tc}^{app} is the effective *trans*-to *cis* isomerization rate in the absence of enzyme while $k_{tc}^{app,SlyD}$ is isomerization rate if the enzyme is bound. Note that those rates are effective rates meaning they are a linear combination of isomerization rates in the folded and unfolded states

because we always have a mixture of folded and unfolded states during the low force quench phase. P_{bound} and $P_{unbound}$ represent the bound and unbound probabilities of SlyD; where P_{bound} is given below and $P_{unbound} = 1 - P_{bound}$;

$$P_{bound} = \frac{[SlyD]}{K_D + [SlyD]} \quad (4)$$

Here [SlyD] corresponds to the concentration of SlyD and K_D represents the dissociation equilibrium constant. The fit to the data in Figure 3d yields $k_{tc}^{app,SlyD}$ = 1.077 ± 0.197 s^{-1}, which is almost two order of magnitude higher compared to enzyme-free isomerization; k_{tc}^{app} = (0.025 ± 0.003) s^{-1} [14]. The estimated dissociation constant is (K_D) is 3.3 ± 1.2 μM, which indicates SlyD as a relatively weak binder to the protein. Notably, the model assumes only one free binding site. Due to the fit is in excellent agreement with the data, we conclude that the catalytic action of SlyD on FLNa20 is a non-cooperative process.

Next, we investigated the force-dependent stability of the folded state (purple state) in the presence and absence of SlyD (Figure 4). An equilibrium experiment at three different forces in the absence of SlyD is shown in Figure 4a. As expected, higher forces shift the equilibrium from the folded to the unfolded state, with the midpoint around 5 pN. In contrast, in the presence of 7.25 uM SlyD the folded probability is strongly increased as compared to the no-SlyD condition (Figure 4b, panel 1). Moreover, the number of unfolding transitions within the *cis*-folded state is reduced compared to the no-SlyD condition. Plotting the force-dependent probability for observing the folded state and the unfolded state (Figure 5) shows a clear SlyD mediated stabilization of the folded state. The midpoint of the transition shifts by around ~2 pN from uncatalyzed (~5 pN) to SlyD catalyzed (~7 pN). This shift corresponds to stabilization by ~2 k_BT of the *cis*-folded state of FlnA20 mediated through SlyD binding.

DISCUSSIONS

In our equilibrium measurements (Figure 2), we find that SlyD concentrations as low as 0.0145 μM already lead to an increase in *trans-cis* isomerization rate by a factor of 2. This observation is in perfect agreement with an enzyme's action, lowering the transition state energy barrier thus speeding up the isomerization kinetics. However, at high concentrations of SlyD there is not obvious further increase of transition rates noticeable in the equilibrium traces (Figure 2, panel 3 and 4). Two effects lead to this observation: first, SlyD seems to stabilize the folded *cis* conformation, thus shifting the equilibrium more to the *cis* state and reducing the number of *cis* unfolded states available for catalysed switching back to the *trans* state. Hence the number of observed transitions goes down. Moreover, the unfolded *trans*-states will become much shorter through the action of the enzyme so that it will be difficult to distinguish whether those states are *trans* states or just short unfolded *cis* states. Previously Žoldák *et al.* [31] reported catalysed isomerization rates of $k_{cis\text{-}trans}$=100/s [31] and $k_{trans\text{-}cis}$=16/s measured on peptides. In fact, a simulation using force-dependent folding/unfolding rates of FlnA20 together with the literature values of SlyD catalysed isomerization rates at a saturating concentration of 7.25 μM shows this effect (Figure S2). Many back and forth isomerization events are observed in phases, where the protein is unfolded thus limiting the resolution of the assay. Hence SlyD will catalyse many forward and backward reactions every second while, in our assay, we use the folding/unfolding kinetics of the protein, which is on the order of seconds at the forces applied to distinguish whether FlnA20 is in a *cis* or in a *trans* state.

As we have already observed a significant acceleration of *trans*-to-*cis* transition rate in the presence of SlyD, separation of two interconnected fast kinetics appears as a big challenge. As the

non-catalysed isomerization is slow, it is easy to separate the slow isomerization rates from fast unfolding/folding rates; individual folded dwell time length is used to discriminate between *cis* and *trans* state. The presence of SlyD accelerates isomerization dramatically, which makes the evaluation of eight different interconnected fast rate constants quite challenging. Previously Žoldák *et al.* showed from stopped-flow experiments, at 7.25μM concentration, the SlyD binding rate is 174 s^{-1} and dissociation rate is 25 s^{-1}. [12a] The catalysed isomerization kinetics was reported on the order of 100 s^{-1}, which indicates that a catalysed back and forth isomerization would happen on the order of 10 ms. Compared to unfolded dwell times, which are on the order of 2 s around 5 pN force bias, we may miss a non-negligible part of isomerization events while FlnA20 is unfolded. Considering this, we still attempted to explore the kinetic information using the jump experiments (Figure 3). Our results from jump experiments agree well with the equilibrium measurements, where we also observed significant lengthening of the *cis*-folded states with SlyD.

The jump experiments (Figure 3) allow a more systematic analysis of the switching kinetics since we can modulate the protein folding/unfolding kinetics by force application. We measure the *trans-cis* isomerization at low forces, where the folding kinetics are fast, and we have a better time resolution to determine the time point when isomerization has happened. It is important to note that, even in this protocol, we are limited by the time the protein needs to refold in the *cis* state, which is on the order of 1s. However, within this time, the enzyme will be able to induce multiple back-and-forth catalysis steps, which we will fail to detect. Hence, the maximum catalysed rate we measure in the jump protocol is only $k_{tc}^{app,SlyD}$=1,077/s, well below the saturation value of 16/s reported by Žoldák *et al.* [31] for RNase T1.

Our experiments clearly show that SlyD, through its catalytic activity, drastically enhances protein folding kinetics into the stable *cis* folded state because it reduces the *trans* lifetime in the

unfolded polypeptide, which lasts for minutes if not catalysed. Previously, Schmid and co-researchers have reported SlyD induced *cis* to *trans* prolyl isomerization of RNAseT1 in bulk, where they also observed an enzymatic effect of SlyD on the folding of this protein.[12a] Unlike our result, they reported a destabilization effect of SlyD through binding to the unfolded polypeptide chain. We observed a stabilization effect for FlnA20, likely through binding to the folded *cis* conformation. It is intriguing that SlyD can work both as a folding kinetics enhancer as well as a stabilizer of the native state. It is important to note that different classes of PPIsomerases have distinct mechanisms of isomerization in different organisms. The effectiveness of enzymatic isomerization also differs vastly depending on the type of enzyme and the protein of choice.

One might also ask why does the native protein gets stabilized in the presence of SlyD. It can be explained by the chaperon domain activity of SlyD. In various studies, the catalytic activity of SlyD as a folding enzyme was investigated by using the reduced and carboxymethylated form of the S54G/P55N variant of RNase-T1 (RCM-T1) as a substrate. [12, 23a, 31] It was reported SlyD alters the folding behaviour of RCM-T1. With the combination of catalytic and chaperon properties, SlyD resembles a trigger factor, a prolyl isomerase that is located at the exit site of the ribosome and is thought to aid in the folding of newly synthesized protein chains. In our case, the chaperon domain of SlyD has caused the same effect, resulting in increased stability of the native *cis* state of the FlnA20 as wells as catalysing the *trans*-to-*cis* isomerization rates.

CONCLUSION

In the current study, we have explored the bacterial SlyD induced *trans*-to-*cis* isomerization of proline 2225 in Filamin A20 (FlnA20). At lower SlyD concentration, two times higher numbers of *trans*-*cis* transitions are observed. This observation infers a clear enzymatic effect of SlyD,

where both of the *trans-cis* and *cis-trans* isomeric transitions increase as SlyD lowers the transition state energy barrier. Moreover, at saturating concentration of SlyD, this observation is changed, where SlyD results in a more prolonged *cis* folded state with a negligible number of transitions to the short-lived *trans* unfolded states. This indicates a possible stabilization of the *cis* folded state in the presence of higher concentrations of SlyD, which agrees well with the chaperon effect of the enzyme. Unfortunately, due to a lack of direct evidence, it's not possible to explore the exact binding mode and the location of the enzyme. Moreover, effective *trans-cis* isomerization rate constant at maximum SlyD concentration has increased by almost 2-orders in magnitude compared to un-enzymatic isomerization in FlnA20. A number of queries related to SlyD are triggered by our experiments, like (a) how many SlyD molecules bind to the FlnA20 at the same time? (b) is SlyD dissociation affected by force? and (c) how is the binding kinetics of SlyD-FlnA20? At this point, answering these questions is beyond our experimental scope as we are only monitoring FlnA20 and changes occurred to its kinetics in the presence of SlyD. A combination of single-molecule force and fluorescence measurement, with fluorophore-labelled SlyD, can be used to answer these questions in the future.

Corresponding Author

[1, *] Technische Universität München
Physik Department
Center for Functional Protein Assemblies (CPA)
Ernst-Otto-Fischer-Str. 8
D-85748 Garching
Germany
Email: matthias.rief@mytum.de

Present Addresses

[2] Gabriel Žoldák
Center for Interdisciplinary Biosciences,
Technology and Innovation Park P.J. Šafárik University,
Trieda SNP 1, 040 11 Košice, Slovakia

Author Contributions

‡ *Equal contribution authors*

Acknowledgement

We strongly acknowledge Tobias Möst's contributions in data collections and analysis processes.

Funding Sources

This work was supported by an Sonderforschungsbereich 863 A2 Grant and ZO 291/1-1 Grant from the Deutsche Forschungsgemeinschaft. M.R. acknowledges financial support through an instrument grant from the Institute for Advanced Study of Technische Universität München. MR has received funding from the European Research Council (ERC) under the European Union's Horizon 2020 research and innovation programme (grant agreement No. 810104 – PoInt).

REFERENCES

1. (a) Brazin, K. N.; Mallis, R. J.; Fulton, D. B.; Andreotti, A. H., Regulation of the tyrosine kinase Itk by the peptidyl-prolyl isomerase cyclophilin A. *Proceedings of the National Academy of Sciences* **2002,** *99* (4), 1899; (b) Mallis, R. J.; Brazin, K. N.; Fulton, D. B.; Andreotti, A. H., Structural characterization of a proline-driven conformational switch within the Itk SH2 domain. *Nature Structural Biology* **2002,** *9* (12), 900-905.
2. Lummis, S. C. R.; Beene, D. L.; Lee, L. W.; Lester, H. A.; Broadhurst, R. W.; Dougherty, D. A., Cis–trans isomerization at a proline opens the pore of a neurotransmitter-gated ion channel. *Nature* **2005,** *438* (7065), 248-252.
3. (a) Eckert, B.; Martin, A.; Balbach, J.; Schmid, F. X., Prolyl isomerization as a molecular timer in phage infection. *Nature Structural & Molecular Biology* **2005,** *12* (7), 619-623; (b) Martin, A.; Schmid, F. X., Evolutionary stabilization of the gene-3-protein of phage fd reveals the principles that govern the thermodynamic stability of two-domain proteins. *J Mol Biol* **2003,** *328* (4), 863-75.
4. Lu, K. P.; Finn, G.; Lee, T. H.; Nicholson, L. K., Prolyl cis-trans isomerization as a molecular timer. *Nature Chemical Biology* **2007,** *3* (10), 619-629.
5. (a) Onuchic, J. N.; Luthey-Schulten, Z.; Wolynes, P. G., THEORY OF PROTEIN FOLDING: The Energy Landscape Perspective. *Annual Review of Physical Chemistry* **1997,** *48* (1), 545-600; (b) Veitshans, T.; Klimov, D.; Thirumalai, D., Protein folding kinetics: timescales, pathways and energy landscapes in terms of sequence-dependent properties. *Folding and Design* **1997,** *2* (1), 1-22.
6. Chakrabarti, S.; Hyeon, C.; Ye, X.; Lorimer, G. H.; Thirumalai, D., Molecular chaperones maximize the native state yield on biological times by driving substrates out of equilibrium. *Proceedings of the National Academy of Sciences* **2017,** *114* (51), E10919.
7. (a) Yaffe, M. B.; Schutkowski, M.; Shen, M.; Zhou, X. Z.; Stukenberg, P. T.; Rahfeld, J.-U.; Xu, J.; Kuang, J.; Kirschner, M. W.; Fischer, G.; Cantley, L. C.; Lu, K. P., Sequence-Specific and Phosphorylation-Dependent Proline Isomerization: A Potential Mitotic Regulatory Mechanism. *Science* **1997,** *278* (5345), 1957; (b) Lu, K. P.; Zhou, X. Z., The prolyl isomerase PIN1: a pivotal new twist in phosphorylation signalling and disease. *Nature Reviews Molecular Cell Biology* **2007,** *8* (11), 904-916; (c) Nicholson, L. K.; Lu, K. P., Prolyl cis-trans Isomerization as a Molecular Timer in Crk Signaling. *Molecular Cell* **2007,** *25* (4), 483-485; (d) Wulf, G.; Finn, G.; Suizu, F.; Lu, K. P., Phosphorylation-specific prolyl isomerization: is there an underlying theme? *Nature Cell Biology* **2005,** *7* (5), 435-441; (e) Andreotti, A. H., Native State Proline Isomerization: An Intrinsic Molecular Switch. *Biochemistry* **2003,** *42* (32), 9515-9524; (f) Fischer, G.; Aumüller, T., Regulation of peptide bond cis/trans isomerization by enzyme catalysis and its implication in physiological processes. In *Reviews of Physiology, Biochemistry and Pharmacology*, Springer Berlin Heidelberg: Berlin, Heidelberg, 2004; pp 105-150; (g) Zhou, X. Z.; Lu, P. J.; Wulf, G.; Lu, K. P., Phosphorylation-dependent prolyl isomerization: a novel signaling regulatory mechanism. *Cell Mol Life Sci* **1999,** *56* (9-10), 788-806.
8. (a) MacArthur, M. W.; Thornton, J. M., Deviations from Planarity of the Peptide Bond in Peptides and Proteins. *Journal of Molecular Biology* **1996,** *264* (5), 1180-1195; (b) Zimmerman, S.

S.; Scheraga, H. A., Stability of Cis, Trans, and Nonplanar Peptide Groups. *Macromolecules* **1976,** *9* (3), 408-416.
9. (a) Steinberg, I. Z.; Harrington, W. F.; Berger, A.; Sela, M.; Katchalski, E., The Configurational Changes of Poly-L-proline in Solution. *Journal of the American Chemical Society* **1960,** *82* (20), 5263-5279; (b) Pincus, M. R.; Gerewitz, F.; Wako, H.; Scheraga, H. A., Cis-trans isomerization of proline in the peptide (his 105-Val 124) of ribonuclease a containing the primary nucleation site. *Journal of Protein Chemistry* **1983,** *2* (2), 131-146; (c) Kang, Y. K., Cis−Trans Isomerization and Puckering of Pseudoproline Dipeptides. *The Journal of Physical Chemistry B* **2002,** *106* (8), 2074-2082.
10. (a) Charbonnier, J. B.; Belin, P.; Moutiez, M.; Stura, E. A.; Quéméneur, E., On the role of the cis-proline residue in the active site of DsbA. *Protein Sci* **1999,** *8* (1), 96-105; (b) Kiefhaber, T.; Grunert, H. P.; Hahn, U.; Schmid, F. X., Replacement of a cis proline simplifies the mechanism of ribonuclease T1 folding. *Biochemistry* **1990,** *29* (27), 6475-6480; (c) Tugarinov, V.; Zvi, A.; Levy, R.; Anglister, J., A cis proline turn linking two beta-hairpin strands in the solution structure of an antibody-bound HIV-1IIIB V3 peptide. *Nat Struct Biol* **1999,** *6* (4), 331-5; (d) Wedemeyer, W. J.; Welker, E.; Scheraga, H. A., Proline Cis−Trans Isomerization and Protein Folding. *Biochemistry* **2002,** *41* (50), 14637-14644.
11. (a) Jakob, R. P.; Schmid, F. X., Energetic coupling between native-state prolyl isomerization and conformational protein folding. *J Mol Biol* **2008,** *377* (5), 1560-75; (b) Pappenberger, G.; Bachmann, A.; Müller, R.; Aygün, H.; Engels, J. W.; Kiefhaber, T., Kinetic Mechanism and Catalysis of a Native-state Prolyl Isomerization Reaction. *Journal of Molecular Biology* **2003,** *326* (1), 235-246; (c) Sarkar, P.; Reichman, C.; Saleh, T.; Birge, R. B.; Kalodimos, C. G., Proline cis-trans Isomerization Controls Autoinhibition of a Signaling Protein. *Molecular Cell* **2007,** *25* (3), 413-426.
12. (a) Zoldák, G.; Geitner, A.-J.; Schmid, F. X., The Prolyl Isomerase SlyD Is a Highly Efficient Enzyme but Decelerates the Conformational Folding of a Client Protein. *Journal of the American Chemical Society* **2013,** *135* (11), 4372-4379; (b) Löw, C.; Neumann, P.; Tidow, H.; Weininger, U.; Haupt, C.; Friedrich-Epler, B.; Scholz, C.; Stubbs, M. T.; Balbach, J., Crystal structure determination and functional characterization of the metallochaperone SlyD from Thermus thermophilus. *J Mol Biol* **2010,** *398* (3), 375-90.
13. (a) Lad, Y.; Kiema, T.; Jiang, P.; Pentikäinen, O. T.; Coles, C. H.; Campbell, I. D.; Calderwood, D. A.; Ylänne, J., Structure of three tandem filamin domains reveals auto-inhibition of ligand binding. *The EMBO Journal* **2007,** *26* (17), 3993-4004; (b) Pentikäinen, U.; Ylänne, J., The Regulation Mechanism for the Auto-Inhibition of Binding of Human Filamin A to Integrin. *Journal of Molecular Biology* **2009,** *393* (3), 644-657; (c) Rognoni, L.; Stigler, J.; Pelz, B.; Ylänne, J.; Rief, M., Dynamic force sensing of filamin revealed in single-molecule experiments. *Proceedings of the National Academy of Sciences* **2012,** *109* (48), 19679.
14. Rognoni, L.; Möst, T.; Žoldák, G.; Rief, M., Force-dependent isomerization kinetics of a highly conserved proline switch modulates the mechanosensing region of filamin. *Proceedings of the National Academy of Sciences* **2014,** *111* (15), 5568.
15. Tolić-Nørrelykke, S. F.; Schäffer, E.; Howard, J.; Pavone, F. S.; Jülicher, F.; Flyvbjerg, H., Calibration of optical tweezers with positional detection in the back focal plane. *Review of Scientific Instruments* **2006,** *77* (10), 103101.

16. Moffitt, J. R.; Chemla, Y. R.; Izhaky, D.; Bustamante, C., Differential detection of dual traps improves the spatial resolution of optical tweezers. *Proceedings of the National Academy of Sciences* **2006,** *103* (24), 9006.
17. (a) Cecconi, C.; Shank, E. A.; Bustamante, C.; Marqusee, S., Direct Observation of the Three-State Folding of a Single Protein Molecule. *Science* **2005,** *309* (5743), 2057; (b) Gebhardt, J. C. M.; Bornschlögl, T.; Rief, M., Full distance-resolved folding energy landscape of one single protein molecule. *Proceedings of the National Academy of Sciences* **2010,** *107* (5), 2013; (c) Stigler, J.; Ziegler, F.; Gieseke, A.; Gebhardt, J. C. M.; Rief, M., The Complex Folding Network of Single Calmodulin Molecules. *Science* **2011,** *334* (6055), 512.
18. Peterman, E. J. G.; Gittes, F.; Schmidt, C. F., Laser-Induced Heating in Optical Traps. *Biophys J* **2003,** *84* (2), 1308-1316.
19. Landry, M. P.; McCall, P. M.; Qi, Z.; Chemla, Y. R., Characterization of Photoactivated Singlet Oxygen Damage in Single-Molecule Optical Trap Experiments. *Biophys J* **2009,** *97* (8), 2128-2136.
20. Kovermann, M.; Schmid, F. X.; Balbach, J., Molecular function of the prolyl cis/trans isomerase and metallochaperone SlyD. *Biological Chemistry* **2013,** *394* (8), 965.
21. Weininger, U.; Haupt, C.; Schweimer, K.; Graubner, W.; Kovermann, M.; Brüser, T.; Scholz, C.; Schaarschmidt, P.; Zoldak, G.; Schmid, F. X.; Balbach, J., NMR Solution Structure of SlyD from Escherichia coli: Spatial Separation of Prolyl Isomerase and Chaperone Function. *Journal of Molecular Biology* **2009,** *387* (2), 295-305.
22. Kaluarachchi, H.; Sutherland, D. E.; Young, A.; Pickering, I. J.; Stillman, M. J.; Zamble, D. B., The Ni(II)-binding properties of the metallochaperone SlyD. *J Am Chem Soc* **2009,** *131* (51), 18489-500.
23. (a) Scholz, C.; Eckert, B.; Hagn, F.; Schaarschmidt, P.; Balbach, J.; Schmid, F. X., SlyD Proteins from Different Species Exhibit High Prolyl Isomerase and Chaperone Activities. *Biochemistry* **2006,** *45* (1), 20-33; (b) Zoldák, G.; Carstensen, L.; Scholz, C.; Schmid, F. X., Consequences of domain insertion on the stability and folding mechanism of a protein. *J Mol Biol* **2009,** *386* (4), 1138-52.
24. (a) Dudko, O. K.; Hummer, G.; Szabo, A., Intrinsic Rates and Activation Free Energies from Single-Molecule Pulling Experiments. *Physical Review Letters* **2006,** *96* (10), 108101; (b) Evans, E.; Ritchie, K., Dynamic strength of molecular adhesion bonds. *Biophys J* **1997,** *72* (4), 1541-1555; (c) Schlierf, M.; Berkemeier, F.; Rief, M., Direct observation of active protein folding using lock-in force spectroscopy. *Biophys J* **2007,** *93* (11), 3989-3998.
25. Bustamante, C.; Marko, J. F.; Siggia, E. D.; Smith, S., Entropic elasticity of lambda-phage DNA. *Science* **1994,** *265* (5178), 1599.
26. Hoffmann, A.; Woodside, M. T., Signal-Pair Correlation Analysis of Single-Molecule Trajectories. *Angewandte Chemie International Edition* **2011,** *50* (52), 12643-12646.
27. (a) Chenna, R.; Sugawara, H.; Koike, T.; Lopez, R.; Gibson, T. J.; Higgins, D. G.; Thompson, J. D., Multiple sequence alignment with the Clustal series of programs. *Nucleic Acids Research* **2003,** *31* (13), 3497-3500; (b) Jagannathan, B.; Elms, P. J.; Bustamante, C.; Marqusee, S., Direct observation of a force-induced switch in the anisotropic mechanical unfolding pathway of a protein. *Proceedings of the National Academy of Sciences* **2012,** *109* (44), 17820; (c) Schwaiger, I.; Schleicher, M.; Noegel, A. A.; Rief, M., The folding pathway of a fast-folding immunoglobulin domain revealed by single-molecule mechanical experiments. *EMBO Rep* **2005,** *6* (1), 46-51.

28. Best, R. B.; Hummer, G., Coordinate-dependent diffusion in protein folding. *Proceedings of the National Academy of Sciences* **2010,** *107* (3), 1088.
29. Brandts, J. F.; Halvorson, H. R.; Brennan, M., Consideration of the possibility that the slow step in protein denaturation reactions is due to cis-trans isomerism of proline residues. *Biochemistry* **1975,** *14* (22), 4953-4963.
30. (a) Schnell, S.; Maini, P. K., Enzyme kinetics far from the standard quasi-steady-state and equilibrium approximations. *Mathematical and Computer Modelling* **2002,** *35* (1), 137-144; (b) Moffitt, J. R.; Chemla, Y. R.; Bustamante, C., Mechanistic constraints from the substrate concentration dependence of enzymatic fluctuations. *Proceedings of the National Academy of Sciences* **2010,** *107* (36), 15739.
31. Zoldák, G.; Schmid, F. X., Cooperation of the Prolyl Isomerase and Chaperone Activities of the Protein Folding Catalyst SlyD. *Journal of Molecular Biology* **2011,** *406* (1), 176-194.

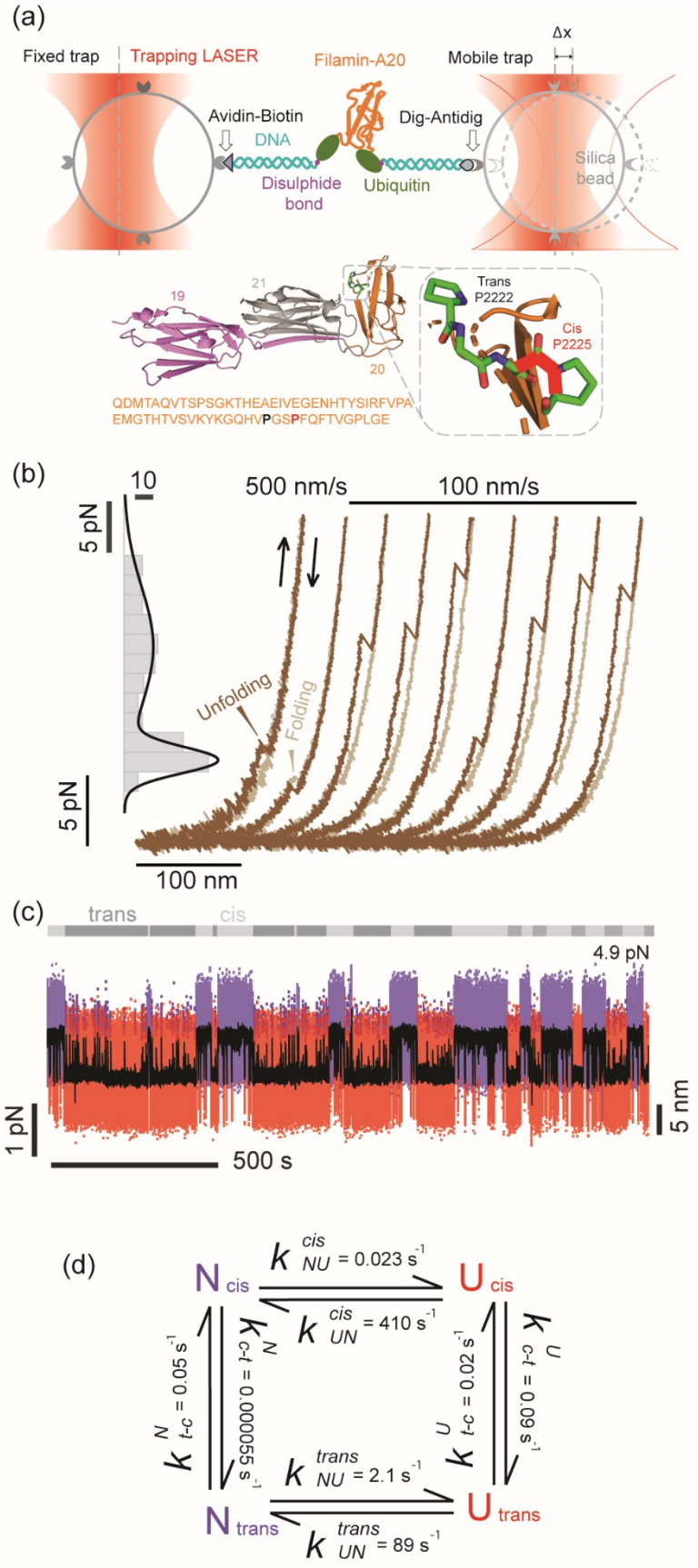
(a)
Fixed trap
Trapping LASER
Filamin-A20
Mobile trap
Δx
Avidin-Biotin
DNA
Dig-Antidig
Disulphide bond
Ubiquitin
Silica bead
19
21
20
Trans P2222
Cis P2225
QDMTAQVTSPSGKTHEAEIVEGENHTYSIRFVPA
EMGTHTVSVKYKGQHVPGSPFQFTVGPLGE
(b)
10
500 nm/s
100 nm/s
5 pN
5 pN
Unfolding
Folding
100 nm
(c)
trans
cis
4.9 pN
1 pN
5 nm
500 s
(d)
N cis
U cis
N trans
U trans
k cis NU = 0.023 s-1
k cis UN = 410 s-1
k N c-t = 0.0000055 s-1
k N t-c = 0.05 s-1
k U t-c = 0.02 s-1
k U c-t = 0.09 s-1
k trans NU = 2.1 s-1
k trans UN = 89 s-1

Figure 1. (a) Schematic of the experimental setup**.** Dumbbell shaped bead-DNA-protein-DNA-bead construct used in dual beam optical tweezer experiments. The DNA is specifically bound to the protein via disulphide bonds and through biotin and digoxygenin to the appropriately functionalized beads (b) Stretch (deep brown) and relax cycles (light brown) of single molecule FLNa20 in absence of SlyD are shown. Left the force distribution is shown in grey histogram, which is fitted using a linear combination of two Gaussian distributions. The scaling of the histogram is shown by black bars at the upper left and top left of the histogram, where the bar marked with 10 represents the amplitude of the histogram. The mean force distribution shows two peaks at 5 pN and 15 pN respectively. (c) Equilibrium time trace of FlnA20 is shown without SlyD, where the force, time and distance scaling are mentioned at the left, bottom and right side respectively. The force bias is at 4.9 pN. The coloured traces correspond to 5 kHz data, where the native folded and unfolded states are marked by purple and red. The black trace is the moving average filtered with 4.2-ms time window. Above the time trace the *cis* and *trans* states of the FlnA20 are marked in the bar using light and dark grey colours respectively. This time trace figure is regenerated using data previously used by Rognoni *et al.* for publication[1]. (d) the four state kinetic model for the folding and prolyl isomerization of FlnA20, where rates are also taken from the previous publication[1].

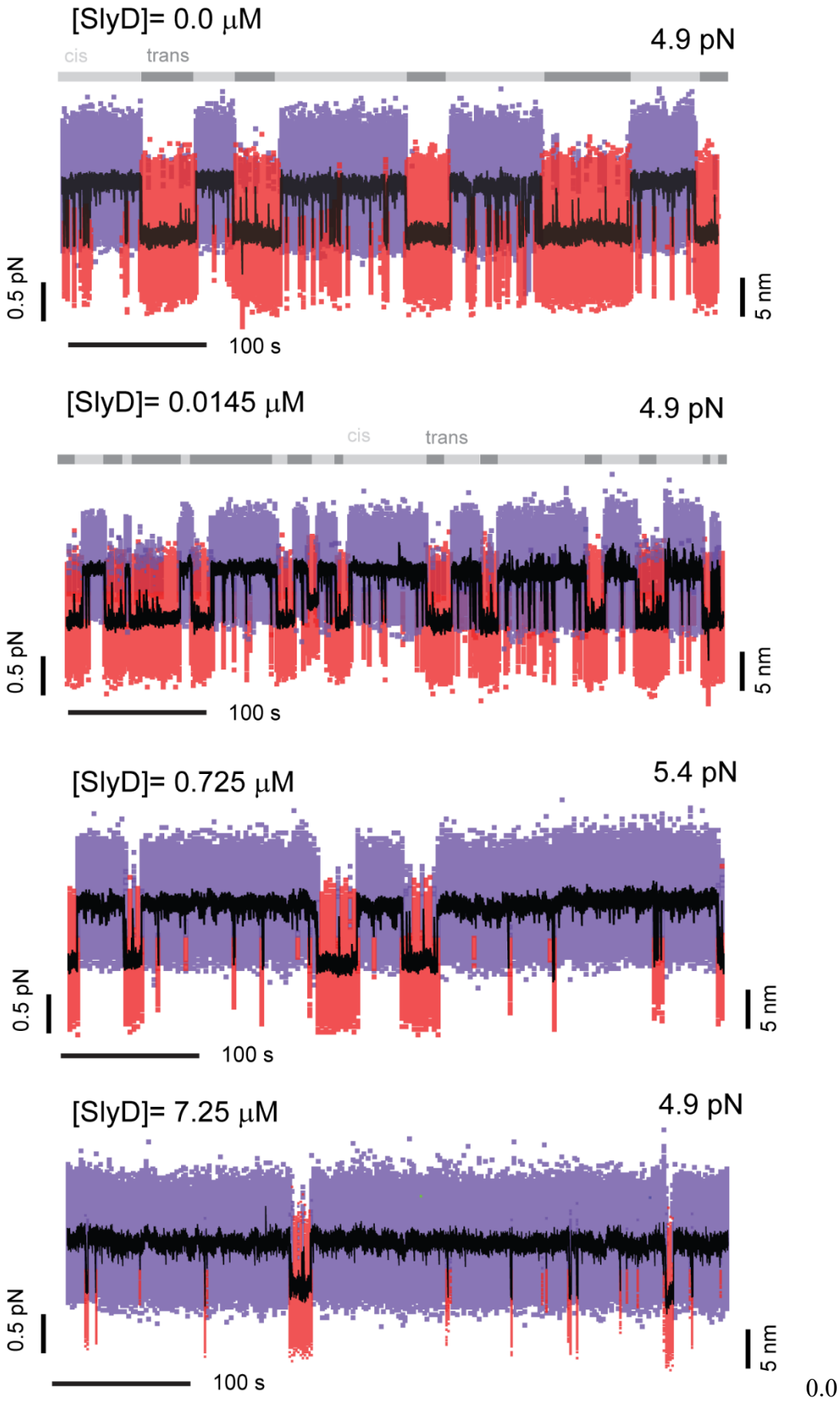
[SlyD]= 0.0 μM
4.9 pN
cis
trans
0.5 pN
5 nm
100 s
[SlyD]= 0.0145 μM
4.9 pN
cis
trans
0.5 pN
5 nm
100 s
[SlyD]= 0.725 μM
5.4 pN
0.5 pN
5 nm
100 s
[SlyD]= 7.25 μM
4.9 pN
0.5 pN
5 nm
100 s

0.0

Figure 2. Comparison of SlyD concentration dependent equilibrium time traces of single FlnA20 molecule, where the concentrations are mentioned above each of the time traces. The force, time and distance scaling are shown respectively at the left, bottom and right side of each panel. A bar above the first and second panels marks the *cis* and the *trans* states in light and dark grey colours respectively. The figure in the first panel is re-produced by using data is from previous publication of Rognoni *et al.*[1] The coloured traces (purple and red) correspond to 5 kHz data, where the native folded and unfolded states are marked by purple and red respectively. The black trace is the moving average filtered with 4.2-ms time window. Above the first two time trace the *cis* and *trans* states of the FlnA20 are marked in the bar using light and dark grey colours respectively.

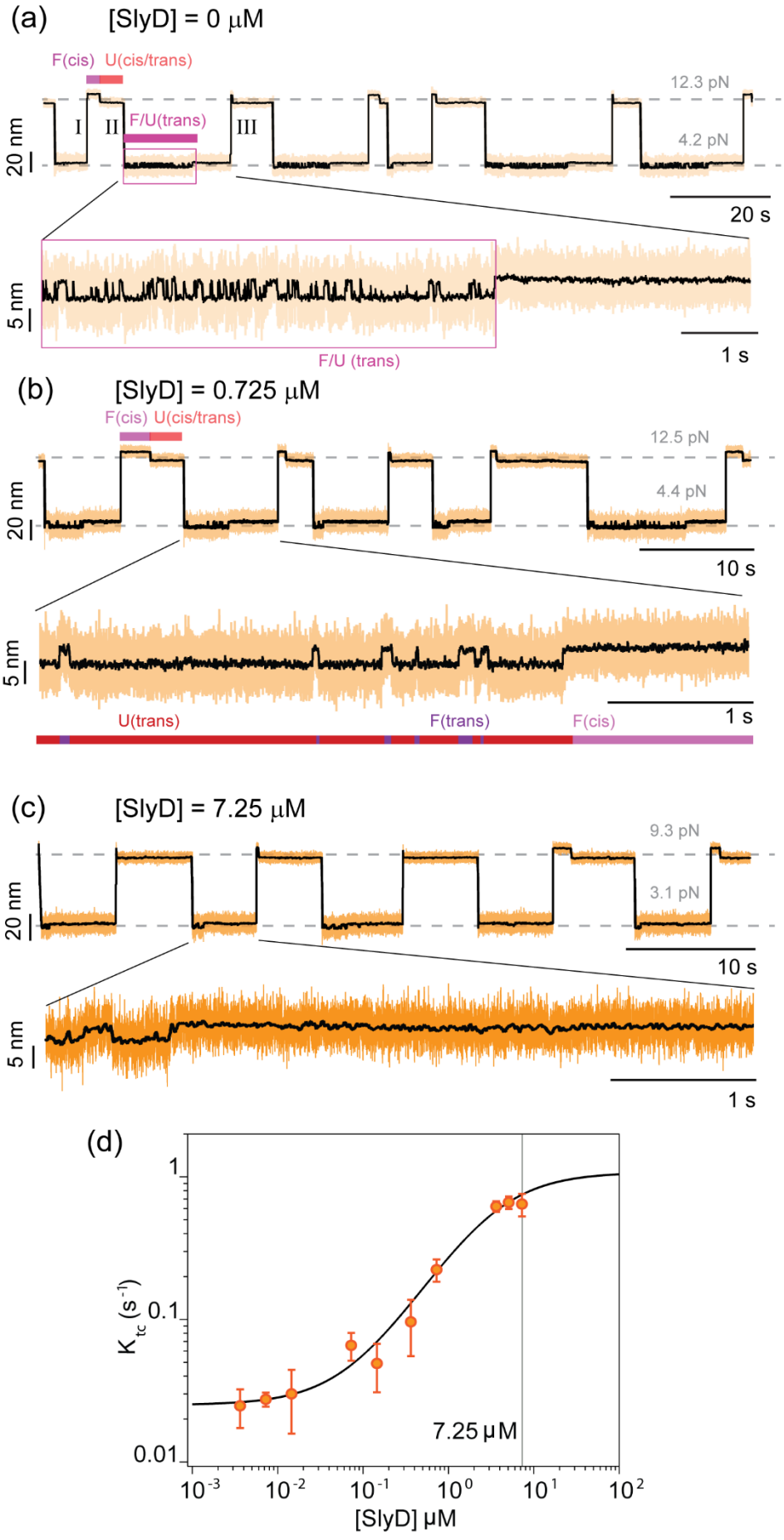
(a)
[SlyD] = 0 μM
F(cis) U(cis/trans)
12.3 pN
4.2 pN
I
II
F/U(trans)
III
20 nm
20 s
5 nm
1 s
F/U (trans)
(b)
[SlyD] = 0.725 μM
F(cis) U(cis/trans)
12.5 pN
4.4 pN
20 nm
10 s
5 nm
1 s
U(trans)
F(trans)
F(cis)
(c)
[SlyD] = 7.25 μM
9.3 pN
3.1 pN
20 nm
10 s
5 nm
1 s
(d)
1
0.1
0.01
K_tc (s^-1)
7.25 μM
10^-3
10^-2
10^-1
10^0
10^1
10^2
[SlyD] μM

Figure 3. Jump experiments (a) without, with (b) 0.725 μM and (c) 7.25 μM of SlyD concentrations are shown, where the mobile trap is jumping between high and low forces. Three different such jump sections are marked by roman numbers (I, II, and III) in the top most trace in (a). Forces between which the trap jumps, are marked by the dotted grey line, and the corresponding value of the force is mentioned above each of the lines. A zoomed in section of each jump traces is shown below each panel, where transitions between *trans*-folded and *trans*-unfolded states can be observed. The orange coloured traces correspond to 5 kHz data, which shows the data collected from the instrument. The black trace is the moving average filtered with 4.2-ms time window. The orange colour intensity increases as the SlyD concentration increases in the experimental assay. In (a) and (b) All the characteristic residence times in the jump experiment are marked by respective colours, like folded *cis* (F(*cis*)) by light purple, unfolded (*cis*/*trans*) (U(*cis*/*trans*)) by light red, unfolded *trans* (U(*trans*)) by deep red, folded *trans* (F(*trans*)) by deep purple and folded or unfolded *trans* (F/U(*trans*)) by magenta colour respectively. A magenta coloured box highlights the folding unfolding region of the *trans* FlnA20 in (a), where repetitive *trans*itions between folded and unfolded states of the *trans* isomer can be observed in the zoomed in section. (d) Effective *trans* to *cis* isomerization rate constant with respect to SlyD concentrations. The effective *trans*-to-*cis* isomerization rate increases with rising SlyD concentration and the data is fitted with a standard binding model, which is described in detail in the text.

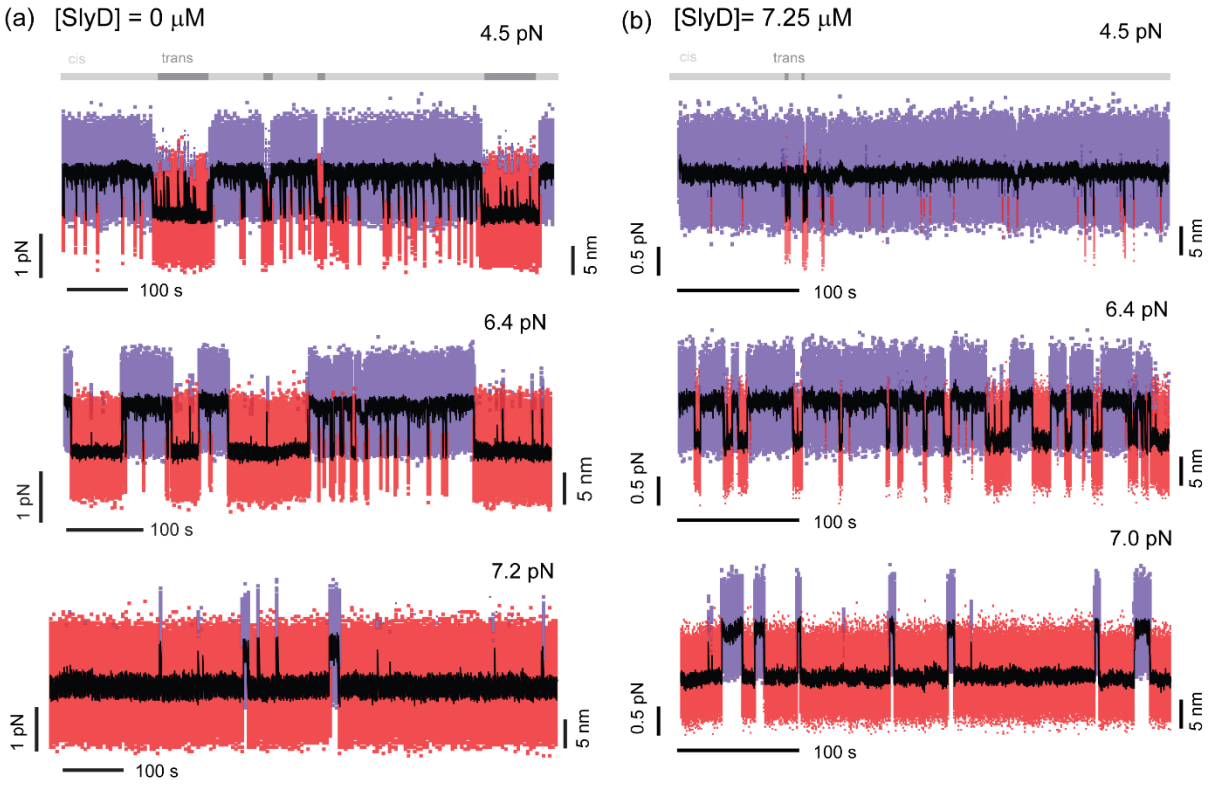

Figure 4. Comparison of force dependent equilibrium time traces of FlnA20; (a) without SlyD and (b) with maximum concentration (7.25 μM) of SlyD. The force bias in each case, which increases from the top to the bottom in each of the columns (a) and (b) is mentioned at the top right corner of the respective panel. Force, time and distance scaling are mentioned respectively at the left, bottom-left and at the right side of each panel. The *cis* and *trans* states are marked by the light and deep grey bars at the top of each column in (a) and (b). The coloured traces (purple and red) correspond to 5 kHz data, where the native folded and unfolded states are marked by purple and red respectively. The black trace is the moving average filtered with 4.2-ms time window.

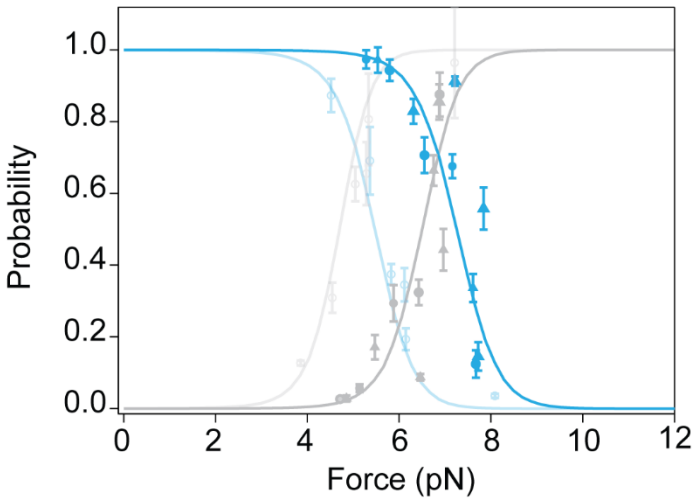

Figure 5. Shows SlyD induced shift in unfolding force midpoint of FlnA20. The blue and grey data points represents folded ((N_{cis} +N_{trans}) / (N_{cis} +N_{trans} + U_{cis} + U_{trans})) and unfolded ((U_{cis} + U_{trans}) / (N_{cis} + N_{trans} + U_{cis} + U_{trans})) probabilities in absence and in presence of 7.25 µM of SlyD. Un-enzymatic data (no SlyD) are shown in faded blue and grey colours, whereas the with SlyD results are shown in deep blue and grey colours. Circles represent data from jump experiments and triangles represent data obtained constant distance equilibrium measurements.

SI Figures

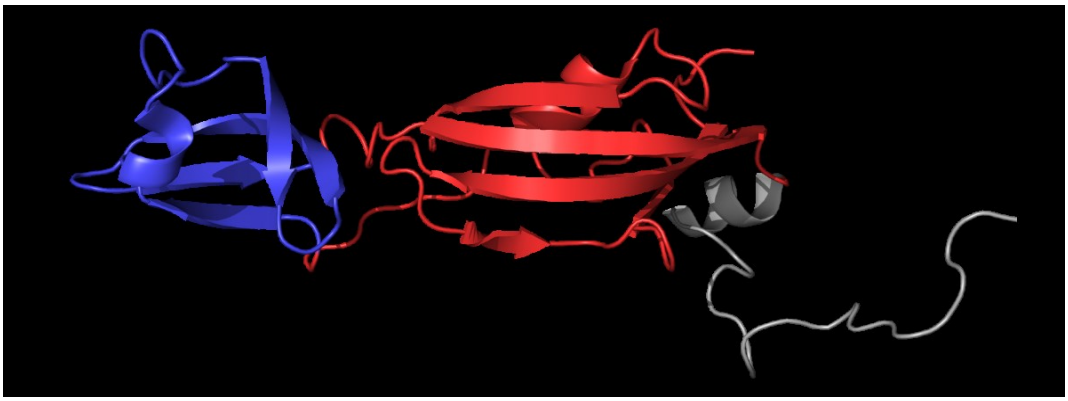

Figure S1. Solution structure (pdbID: 2K8I) of peptidyl-prolyl *cis*/*trans* isomerase SlyD. The upper chaperone domain is coloured in blue while the lower isomerase domain is depicted in red. The grey coloured domain contains multiple histidine which binds to Ni^{+2} ions and hinder the isomerase activity.

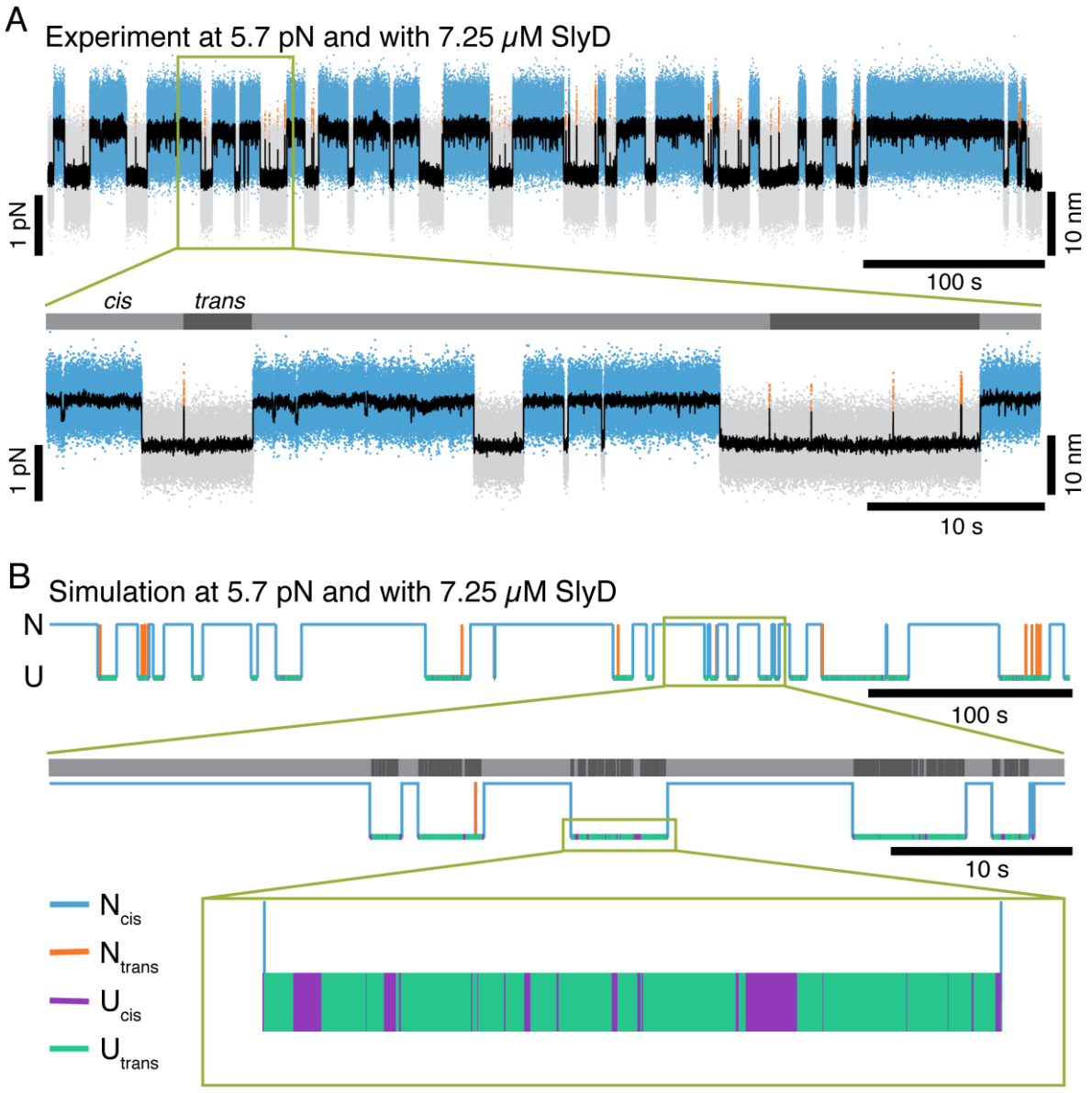

Figure S2: Comparison of an equilibrium measurement time trace collected at highest concentration (7.25μM SlyD) of SlyD with a corresponding Monte-Carlo simulation. (A) Equilibrium measurement time trace was collected at a force bias of 5.7pN and with 7.25μM SlyD (upper panel). In lower panel a zoom in view of a representative region with *cis* and *trans* folded dwells. The isomerization state assignment is given by the light and dark grey line above the zoom. (B) Monte-Carlo simulation of a passive-mode experiment taken at the same conditions as (A). Upper panel shows full-length 500s time trace with color-coding (shown in the legend) for N_{cis}, U_{cis}, N_{trans} and U_{trans}. The SlyD-bound states were lumped into the unfolded states. Middle panel shows a zoom view of the green marked region of a full-length trace. The zoomed view in the lowest panel shows a high frequency switching between *cis* and *trans* while the protein is unfolded.

1. Rognoni, L.; Möst, T.; Žoldák, G.; Rief, M., Force-dependent isomerization kinetics of a highly conserved proline switch modulates the mechanosensing region of filamin. *Proceedings of the National Academy of Sciences* **2014,** *111* (15), 5568.

TOC Graphic

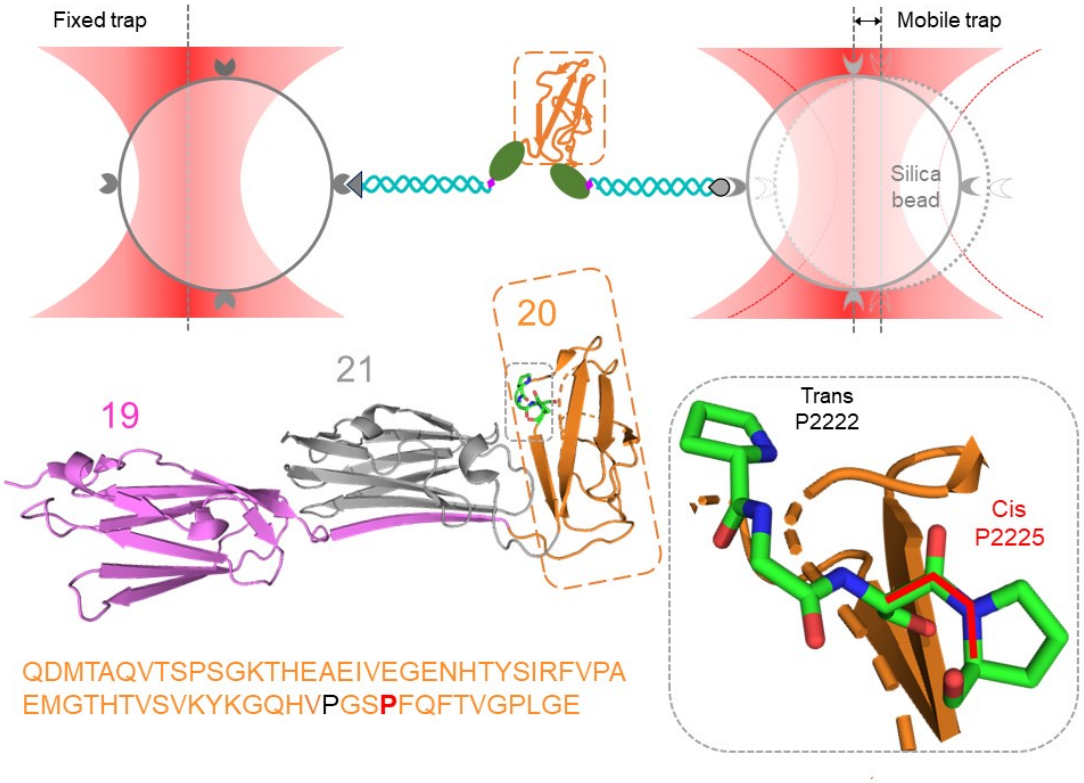
Fixed trap
Mobile trap
Silica bead
20
21
19
Trans
P2222
Cis
P2225
QDMTAQVTSPSGKTHEAEIVEGENHTYSIRFVPA
EMGTHTVSVKYKGQHVPGSPFQFTVGPLGE